Proc. Indian Acad. Sci., Vol. 85 A, No. 4, 1977, pp. 218–229.

Rotating hydromagnetic free shear layer flow for very large magnetic interaction parameter*

SOMARAJU VEMPATY

Department of Mathematics, PSG College of Technology, Coimbatore 641004

MS received 2 July 1976; after revision 22 September 1976

ABSTRACT

The hydromagnetics of a linear, steady, axisymmetric flow of an electrically conducting homogeneous fluid confined between two identical rotating electrically insulated parallel plates are analysed for a free shear layer situation when $\alpha^2 \gg E^{-1/3}$ where α^2 is the rotational magnetic interaction parameter and E is the Ekman number. A few cases involving subtle changes of the imposed azimuthal velocity boundary condition are solved to elucidate the meridional electric current flow.

1. INTRODUCTION

KNOWLEDGE of hydromagnetic boundary layers in rotating flows plays an important role in the understanding of various astrogeophysical flows. Vempaty and Loper[1] have analysed the side wall hydromagnetic boundary layers in a steadily rotating electrically insulated cylindrical container using the singular perturbation techniques. The analysis covered completely the two parametric ranges of the magnetic interaction parameter, $\alpha^2 \,(=\sigma b^2/2\rho\Omega)$ which measures the ratio between the magnetic force and the Coriolis force. If $E\,(=\nu/\Omega L^2)$ denotes Ekman number which measures the ratio between the viscous and Coriolis force, it was shown that all the vertical shear layers that occur for $\alpha^2 \ll E^{-1/3}$ merge together to form a single layer as $\alpha^2 \to E^{-1/3}$, and this layer has a thickness $O\,(E^{1/4}\alpha^{-1/2})$ for $\alpha^2 \gg E^{-1/3}$. The rotational forces become unimportant in this extreme range.

In this paper, we shall choose a simple free shear layer situation (*see* section 2) and analyse for $\alpha^2 \gg E^{-1/3}$ the hydromagnetics in various regions of interest with a special emphasis on the vertical shear layer structure.

* A part of the Ph.D. Dissertation submitted to Florida State University, Tallahassee, USA.

In section 2, we give a description of the problem and its mathematical formulation. The analysis of the various regions of flow is given in section 3, and finally the comments and conclusions appear in section 4.

2. MATHEMATICAL FORMULATION

The geometry of the free shear layer situation considered here is exactly the same as that considered by Greenspan.[2] Consider a conducting fluid confined between two electrically insulated identical parallel plates separated by a distance L and rotating uniformly about the axis of symmetry with an angular velocity $\vec{\Omega}$ under the influence of a uniform magnetic field applied in the same direction as the angular velocity vector. An inner disc of radius R attached to each plate can spin independently. Fluid motions away from the state of solid body rotation are produced by imposing a small, steady perturbation in angular velocity $\epsilon\Omega$ on the bottom inner disc, and $\pm\,\epsilon\Omega$ (the plus sign corresponds to the "symmetric case" and the minus sign the "antisymmetric case") on the upper inner disc (*see* figure 1).

Under the assumptions that the Rossby number and the magnetic Reynolds number are small, the non-dimensional governing equations for the steady state situation considered above are the same as equations (8) given in reference 1. Since we are mainly interested in regions E and F [That is regions near $r = a$ $(= R/L)$ where r is the non-dimensional radial distance, and a is the aspect ratio], the curvature terms can be neglected in the above-said equations. The equations then become,

$$2v_z = 2a^2\psi_{zz} - E\nabla^2\psi \tag{1}$$

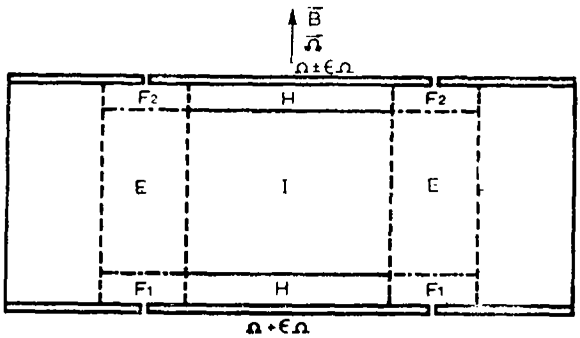

Figure 1. A diagram showing the various regions of flow in the concentric disc free shear layer configuration. The boundaries whose angular velocities are not marked in the figure are supposed to be rotating with angular velocity Ω. I: Interior region; H: Ekman-Hartmann layer; E: Vertical boundary layer; F: Ekman-Hartmann extension of the vertical boundary layer.

$$2\psi_z = 2a^2 b_z + E\nabla^2 v \tag{2}$$

$$v_z + \nabla^2 b = 0 \tag{3}$$

where a subscript denotes differentiation, and

$$\nabla^2 = \frac{\partial^2}{\partial x^2} + \frac{\partial^2}{\partial z^2} \quad \text{and} \quad x = a - r.$$

Here, v denotes the azimuthal velocity, b the azimuthal magnetic field which also serves as a steam function for the electric currents, ψ the steam function for the meridional flow, α^2 the magnetic interaction parameter, and E the Ekman number.

The boundary conditions on velocity field may be written as

$$v = f(x) = r\delta(x) \qquad \text{at } z = 0$$

$$v = \pm f(x) = \pm r\delta(x) \qquad \text{at } z = 1$$

$$\psi = 0 \qquad \text{at } z = 0, 1$$

where δ is a unit step function. Since the plates are electrically insulated, the electric current flux normal to the boundaries is zero and hence by Ampere's law

$$b = 0 \quad \text{at } z = 0, 1.$$

From (2)–(3) it directly follows that the thickness of the horizontal boundary layer (hereafter referred as Ekman-Hartmann layer) is $O(M^{-1})$ and the thickness of the vertical layer is $O(M^{-1/2})$ where M is the Hartmann number given by $M = E^{-1/2}\alpha$. It also follows from (1)–(3) that in both the layers

$$v = O(1), \qquad b = O(E^{1/2}\alpha^{-1}), \qquad \text{and} \qquad \psi_z = \alpha^{-2}.$$

Hence, the Coriolis term is insignificant to dominant order in the zonal momentum equation (2). As a result, equations (2) and (3), containing only the variables v and b decouple from the first equation and they may be written as,

$$v_{xx} + v_{zz} + M\hat{b}_z = 0 \tag{4}$$

$$\hat{b}_{xx} + \hat{b}_{zz} + Mv_z = 0 \tag{5}$$

where

$$\hat{b} = Mb.$$

We may rewrite the above equations as

$$R_{xx} + R_{zz} + MR_z = 0 \tag{6}$$

$$S_{xx} + S_{zz} - MS_z = 0 \tag{7}$$

where

$$R = v + \hat{b} \quad \text{and} \quad S = v - \hat{b}. \tag{8}$$

The boundary conditions on R and S become

$$\left.\begin{array}{ll} R = S = rf(x) & x > 0 \\ R = S = 0 & x < 0 \end{array}\right\} \text{ at } z = 0 \tag{9}$$

$$\text{At } z = 1 \quad R = S = \begin{cases} rf(x) \text{ Sym.} & x > 0 \\ -rf(x) \text{ Antisym.} & x > 0 \end{cases} \tag{10}$$

$$\text{At } z = 1 \quad R = S = 0 \qquad x < 0.$$

Equations (6) and (7) should now be solved subject to boundary conditions (9) and (10).

Since the boundary layer contributions vanish at the edge of the boundary layers, the unstretched boundary layer co-ordinate may be allowed to range between $+\infty$ and $-\infty$. The problem now becomes amenable to Fourier transformation in x.

3. Mathematical Analysis

Define the Fourier integral tansform pair for any variable ϕ as

$$\bar{\phi}(\xi) = \int_{-\infty}^{+\infty} \phi(x) \cdot \exp(-i\xi x)\, dx$$

$$\phi(x) = \frac{1}{2\pi} \int_{-\infty}^{+\infty} \bar{\phi}(\xi) \cdot \exp(i\xi x)\, d\xi.$$

Fourier transformation of equations (6) and (7) gives us

$$\bar{R}_{zz} + M\bar{R}_z - \xi^2 \bar{R} = 0 \tag{11}$$

$$\bar{S}_{zz} - M\bar{S}_z - \xi^2 \bar{S} = 0. \tag{12}$$

Antisymmetric case

Solution for the vertical boundary layer (Region E);

The solution of (11) subject to boundary condition (9)–(10) is

$$\bar{R} = \frac{\bar{f}(\xi)\,[\exp\{-(M/2)(1 - z)\} \sinh(\mu z) + \exp\{-(M/2) z\} \cdot \sinh \mu (1 - z)]}{\sinh \mu} \tag{13}$$

where

$$\mu = \left(\xi^2 + \frac{M^2}{4}\right)^{\frac{1}{2}}$$

since $\mu \gg 1$, $\sinh \mu \simeq e^{\mu}$. Therefore (13) may be written as

$$\bar{R} \simeq -\bar{f}(\xi) \exp\{M/2\,(1-z)\}\,[\exp\{-\mu(1-z)\} - \exp\{-\mu(1+z)\}]$$
$$+ \bar{f}(\xi)\cdot\exp(-Mz/2)\,[\exp(-\mu z) - \exp -\{\mu(2+z)\}]. \quad (14)$$

Away from regions of thickness $O(M^{-1})$ near the walls $z = 0, 1$ (*i.e.*, in region E), only the first term of (14) is significant. Therefore, in region E

$$R \simeq \frac{-a \exp\{(M/2)(1-z)\}}{2\pi i} \int_{-\infty}^{+\infty} \frac{\exp(ix\xi)\cdot\exp\{-\mu(1-z)\}}{\xi}\,d\xi. \quad (15)$$

where $\bar{f}(\xi)$ is replaced by $a/i\xi$ with the understanding that the solutions are sought for $x \ll 1$ and the pole due to $\xi = 0$ contributes only to the region $x > 0$. (a should be replaced by r in the final solutions to obtain a proper representation of the flow dynamics.) Following the method used by Hunt and Williams[3] to solve almost a similar integral as (15), (the only difference is that the pole $\xi = 0$ contributes only to the region $x > 0$ in our case, while it contributes to both the regions $x > 0$ and $x < 0$ in their case) we write

$$2\xi = M \sinh(\theta + i\psi).$$

Then (15) becomes

$$R \simeq -\frac{a}{2\pi i} \exp[M(1-z)/2] \int_{-\infty-i\psi}^{\infty-i\psi} \exp(-\tfrac{1}{2} Mt \cosh\theta) \coth(\theta + i\psi)\,d\theta \quad (16)$$

where $t^2 = (1-z)^2 + x^2$ and $\tan\psi = x/(1-z)$. Evaluating the contribution of the pole $\theta = -i\psi$ for the region $x > 0$, we have

$$R \simeq -\frac{a}{2\pi i} \exp\,[M(1-z)/2] \int_{-\infty}^{+\infty} \exp(Mt/2 \cosh\theta) \coth(\theta + i\psi)\,d\theta$$
$$-\,a\delta(\psi) \quad (17)$$

where δ is the heavy-side unit step function. Evaluation of (17) gives,

$$R \simeq -\frac{a}{2}\frac{\cos\psi}{\cos(\psi/2)}[\operatorname{erfc}\{-(Mt)^{1/2} \sin\psi/2\} - 2\delta(\psi)] - a\delta(\psi). \quad (18)$$

Equation (18) is valid for all ψ. Since in region E, $x = O(M^{-1/2})$ and $(1-z) \gg x$, we have

$$\cos\psi \simeq \cos\psi/2 \simeq 1, \quad t \simeq (1-z), \sin(\psi/2) \simeq \frac{x}{2(1-z)}$$

Therefore

$$R \simeq -\frac{a}{2} - \frac{a}{2}\,\mathrm{erf}\left(\frac{M^{1/2}x}{2(1-z)^{1/2}}\right) \tag{19}$$

Similarly

$$S \simeq \frac{a}{2} + \frac{a}{2}\,\mathrm{erf}\left(\frac{M^{1/2}x}{2z^{1/2}}\right). \tag{20}$$

From (19)–(20) and by (8) we get

$$v = \frac{a}{4}\,\mathrm{erf}\left(\frac{M^{1/2}x}{2z^{1/2}}\right) - \frac{a}{4}\,\mathrm{erf}\left(\frac{M^{1/2}x}{2(1-z)^{1/2}}\right) \tag{21}$$

$$b = -\left[\frac{a}{2} + \frac{a}{4}\,\mathrm{erf}\left(\frac{M^{\frac{1}{2}}x}{2z^{1/2}}\right) + \frac{a}{4}\,\mathrm{erf}\left(\frac{M^{\frac{1}{2}}x}{2(1-z)^{1/2}}\right)\right]. \tag{22}$$

These solutions contain the combination of interior and boundary layer contributions. The boundary layer contributions can be obtained by subtracting the respective interior solutions. Taking the limit as $x \to \infty$ it is seen from (21)–(22) that $v = 0$ and $b = -r$ (a is replaced by r to get the correct representative solution) in the interior region I. For $x < 0$, the interior solutions for both v and b are zero as should be expected physically from the nature of the boundary conditions for $x < 0$.

SOLUTION FOR THE REGION F_1:

In the vicinity of $z = 0$, the first three terms in (14) are important. Hence in region F_1, we get

$$R \simeq -\frac{a}{2\pi i}\exp\left[M(1-z)/2\right] \int_{-\infty}^{+\infty} \frac{\exp(ix\xi)\left[\exp\{-\mu(1-z)\} - \exp\{-\mu(1+z)\}\right] d\xi}{\xi}$$
$$+ \frac{a}{2\pi i}\exp-[Mz/2] \int_{-\infty}^{+\infty} \frac{\exp(ix\xi)}{\xi} \cdot \exp(-\mu z)\, d\xi. \tag{23}$$

The integrands of (23) are similar to the integrands of (15); we shall write the solution for (23) by inspection of (15) and its solution (18).

$$R \simeq -\left[\frac{a}{2}+\frac{a}{2}\operatorname{erf}\left(\frac{M^{1/2}x}{2(1-z)^{1/2}}\right)\right]$$

$$+\exp(-Mz)\left[\frac{a}{2}+\frac{a}{2}\operatorname{erf}\left(\frac{M^{1/2}x}{2(1+z)^{1/2}}\right)\right.$$

$$+\exp(-Mz)\left[\frac{a}{2}+\frac{a}{2}\operatorname{erf}\left(\frac{M^{1/2}x}{2z^{1/2}}\right)\right]$$

Since $z \sim O(M^{-1})$ in the region under consideration, we may replace z with zero in the error functions occurring in the first two terms and the error function in the last term may be replaced by $\pm\delta(\pm x)$. [For $x>0$, this is equivalent to $+\delta(+x)$ and for $x<0$ to $-\delta(-x]$. Finally we obtain

$$R \simeq \exp(-Mz)\left[\frac{a}{2}\pm\frac{a}{2}\delta(\pm x)\right]-\frac{a}{2}\left[1-\exp(-Mz)\right]\operatorname{erf}(M^{1/2}x/2)$$

$$-\frac{a}{2}\left[1-\exp(-Mz)\right] \tag{24}$$

Similarly

$$S \simeq \frac{a}{2}+\frac{a}{2}\operatorname{erf}\left(\frac{M^{1/2}x}{2z^{1/2}}\right). \tag{25}$$

However, in the region F_1, since $z \sim O(M^{-1})$ and $x \sim O(M^{-\frac{1}{2}})$, the order of $M^{1/2}x/z^{1/2}$ is $M^{1/2}$ which is very large. Therefore, the error function in (25) can be replaced by $\pm\delta(\pm x)$. Hence

$$S \simeq a \qquad x>0$$

$$\simeq 0 \qquad x<0. \tag{26}$$

This says that the variable $S(=v-b)$ does not have a boundary layer structure near $z=0$. This does not mean that v and b cannot have boundary layer structures near $z=0$. This boundary layer contributions for v and b can be directly obtained from (24) and (26).

It is instructive to obtain the solution of the Ekman-Hartmann layer region H, from (24) and (26). As $x\to\infty$ we have

$$R = v+b = -a+2a\exp(-Mz)$$

$$S = v-b = a$$

Hence

$$v = a\exp(-Mz)$$

$$b = -a+a\exp(-Mz)$$

which are the solutions for v and b in the region H_1 for the antisymmetric case when a is replaced by r.

It is now a routine matter to find the solutions for the region F_2 at $z = 1$ The analysis would show that R does not possess a boundary layer structure near $z = 1$ while S will have.

The mathematical method being exactly the same, we shall now directly write down the solutions for the vertical shear layer region E for the symmetric and mixed cases. The mixed case which is neither symmetric nor antisymmetric has the boundary conditions.

$v = r\delta(x)$ at $z = 0$, $v = 0$ at $z = 1$ and

$b = 0$ at $z = 0, 1$.

SOLUTION FOR REGION E IN THE SYMMETRIC CASE:

$$v \simeq \frac{a}{2} + \frac{a}{4}\operatorname{erf}\left(\frac{M^{1/2}x}{2z^{1/2}}\right) + \frac{a}{4}\operatorname{erf}\left(\frac{M^{1/2}x}{2(1-z)^{1/2}}\right) \tag{27}$$

$$b \simeq \frac{a}{4}\operatorname{erf}\left(\frac{M^{1/2}x}{2(1-z)^{1/2}}\right) - \frac{a}{4}\operatorname{erf}\left(\frac{M^{1/2}x}{2z^{1/2}}\right) \tag{28}$$

SOLUTION FOR REGION E IN THE MIXED CASE:

$$v \simeq \frac{a}{4} + \frac{a}{4}\operatorname{erf}\left(\frac{M^{1/2}x}{2z^{1/2}}\right) \tag{29}$$

$$b \simeq -\frac{a}{4} - \frac{a}{4}\operatorname{erf}\left(\frac{M^{1/2}x}{2z^{1/2}}\right). \tag{30}$$

The boundary layer contributions $\tilde{v}$ and $\tilde{b}$ for $x < 0$ are the same as above. For $x > 0$, these are

$$\tilde{v} \simeq -\frac{a}{4}\operatorname{erfc}\left(\frac{M^{1/2}x}{2z^{1/2}}\right) \tag{31}$$

$$\tilde{b} \simeq \frac{a}{4}\operatorname{erfc}\left(\frac{M^{1/2}x}{2z^{1/2}}\right). \tag{32}$$

4. COMMENTS AND CONCLUSIONS

First we would like to say a few words about the equations (4)–(7) and the solutions obtained. These equations are elliptic equations. However, it may be seen that in the vertical shear layer, since $\partial/\partial x \gg \partial/\partial z$, the equations (6)–(7) reduce to the parabolic equations,

$$R_{xx} + MR_z = 0$$

$$S_{xx} - MS_z = 0.$$

The solutions we obtained in section 3 for R and S in the side boundary layer are in fact the solutions of the above parabolic equations. Hence, the side boundary layer may be called a parabolic boundary layer.

It may be seen from the solutions obtained here for the free shear layer region, that its essential dynamics are the same as that of the side wall boundary layer analysed in reference (1) for $\alpha^2 \gg E^{-1/3}$. This is in general true, and so the analysis of a suitable free shear layer situation may prove helpful in analysing certain complicated boundary layer problems which demand a proper insight into the physical situation.

It is known from earlier work[4] that the vertical shear in the azimuthal velocity of the Ekman-Hartmann layer gives rise to a radial electric current in that region and hence by continuity to an axial current in the interior. In what follows, we shall discuss the circulation of this electric current flux in all the three cases considered in section 3.

The electric current flow pattern for the antisymmetric, symmetric, and mixed cases is shown schematically in figures 2–4. It may be seen from the solutions obtained, that for the antisymmetric case, half of the electric current flux pumped by the Ekman-Hartmann layer H, enters the region E, directly from regions F_1 while the other half enters through the corner region (*see* figure 2).

In the symmetric case, the interior region itself can satisfy the boundary conditions at $z = 0$, 1 [follows directly from equations (27–28)] and hence there is no Ekman-Hartmann layer. The electric current flow through the interior vanishes. However, the electric currents flow near the region $x = 0$ and are confined to the boundary layer regions E and F. The electric currents circulate as four separate cells partitioned by $x = 0$ and $z = \frac{1}{2}$ (*see* figure 3).

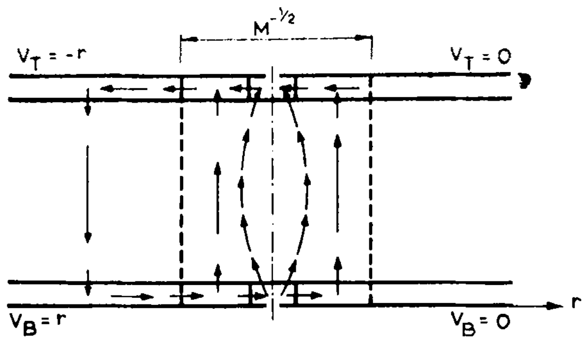

Figure 2. A schematic diagram of the meridional electric current flow in the antisymmetric case. The arrows indicate the electric current flux O $(E^{1/2}/\alpha)$.

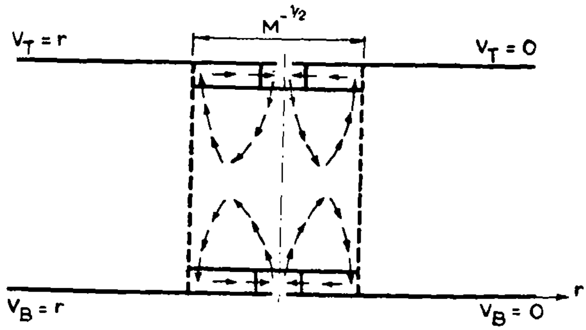

Figure 3. A schematic diagram of the meridional electric current flow in the symmetric case. The arrows indicate the electric current flux $O(E^{1/2}/\alpha)$.

In the mixed case, since $\tilde{b} = 0$ at $z = 0$ by equation (32), the electric currents cannot directly enter into the region E. They enter into this region only through the corner region. This result may also be understood physically, if we realise that the mixed case is a combination of symmetric and antisymmetric cases. In symmetric case the region F_1 sucks electric currents from the region E, while in the antisymmetric case, the reverse happens. Hence, it may be thought, that in the mixed case, the electric current can manage to enter the region, E only through the corner region. In fact, not only $\tilde{b}$, but also $\tilde{v}$ is zero at $z = 0$. This observation leads us to conclude (can be shown by analysis also[5]) that the region F_1 does not exist in this case.

Having known v, the solution for the field variable ψ can be obtained from (1) in principle. As noted in reference (1), the solution for ψ involves resonance and is complicated and unilluminating. However, we can draw certain conclusions regarding the circulation of mass flux from the order of magnitude analysis. It follows from equation (1) that $\psi \sim O(E^{1/2}\alpha^{-3})$ in the regions, I, H and F. Since $\psi \sim O(\alpha^{-2})$ in the region E, an intense circulation of mass flux $O(\alpha^{-2})$ takes place in this region. The interior mass flux being of very small magnitude need not be considered.

Finally we shall summarise the results commenting on the effect of magnetic field on a rotating flow, and explaining briefly the major changes that ensue when the magnetic interaction parameter becomes very large. It is seen that the thickness of the boundary layers decrease as the magnetic field increases. Obviously, this is because, that, as the magnetic forces increase, the viscous forces have to increase to balance them. As a result, the thickness of the layer has to decrease. It is known from earlier work[4] (and also can be seen from the magnitudes of ψ and b in the horizontal

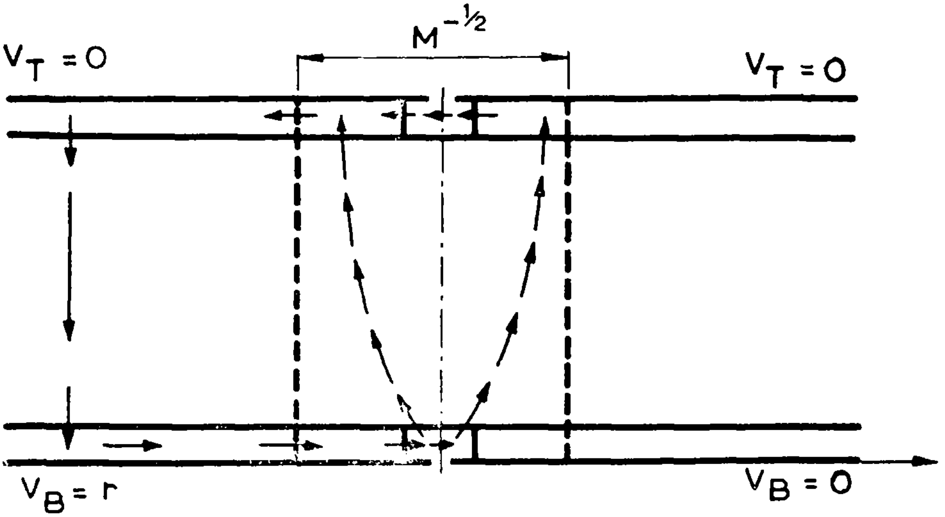

Figure 4. A schematic diagram of the meridional electric current flow in the mixed case. The arrows indicate the electric current flux $O\ (E^{1/2}/\alpha)$.

boundary layer) that due to the presence of magnetic field, an axial current is induced while the axial mass flux is inhibited. The side boundary layers that occur should be able to support this electric current flux as well as the mass flux pumped by the horizontal boundary layer. It was shown[1] that for $\alpha^2 \ll E^{-1/3}$, in addition to two non magnetic layers (which are exactly similar to the Stewartson's $E^{1/3}$ and $E^{1/4}$ layers that occur in a nonmagnetic rotating flow) which support the mass flux, there occur two hydromagnetic layers to support the electric current. In all these layers the Coriolis forces are important. However, as $\alpha^2 \to E^{-1/3}$ the magnetic, the viscous and the Coriolis forces assume the same magnitude and as a result all the different layers merge together to form a single layer. For $\alpha^2 > E^{-1/3}$ the rotational forces become unimportant, and the essential dynamics of the single side layer are determined by a balance between the magnetic and viscous forces. This layer attains a parabolic structure characteristic of strongly magnetic non rotational flows.

ACKNOWLEDGEMENTS

The author is grateful to Dr. David E. Loper, GFDI, Florida State University, USA, for his valuable guidance during the course of this work. This work was supported in part by the National Science Foundation No. GA-18853 and in part by the Office of Naval Research, USA, under contract No. 00014-A-0159.

REFERENCES

1. Vempaty, S. and Loper, D. E., *Phys. Fluids* **18** 1678 (1975).
2. Greenspan, H. P., *The Theory of Rotating Fluids*, Cambridge University Press, p. 101 (1968).
3. Hunt, J. C. R. and Williams, W. E., *J. Fluid Mech.* **31** 705 (1968).
4. Gilman, P. A. and Benton, E. R., *Phys. Fluids* **11** 2397 (1968).
5. Vempaty, S. *Hydromagnetic Boundary Layers in Rotating Flows* Ph.D. Dissertation, Florida State University (1974).